European Journal of Radiology 119 (2019) 108652

Contents lists available at ScienceDirect

European Journal of Radiology

journal homepage: www.elsevier.com/locate/ejrad

A feasibility study of pulmonary nodule detection by ultralow-dose CT with adaptive statistical iterative reconstruction-V technique

Kai Ye, Qiao Zhu, Meijiao Li, Yuliu Lu, Huishu Yuan*

Department of Radiology, Peking University Third Hospital, Beijing, China

ARTICLE INFO

Keywords:
Ultralow-dose
Pulmonary nodule
Computed tomography
ASiR-V
Lung cancer screening

ABSTRACT

Purpose: To evaluate the clinical value of ultralow-dose CT (ULDCT) with adaptive statistical iterative reconstruction-V (ASiR-V) in the detection of pulmonary nodules in a Chinese population.

Method: One hundred eighty-eight patients (16.41 ≤ BMI ≤ 29.87 kg/m^2) with pulmonary nodules detected on low-dose chest CT (LDCT) underwent local ULDCT at the center of the chosen nodule with a scan length of 3 cm. LDCT was performed using the Assist kV (120/100 kV)/Smart mA mode and at 120 kV/2.8 mAs for ULDCT. After scanning, CT images were reconstructed with ASiR-V 50%. For both scans, nodule diameters were measured and reference standards were established for the presence and types of lung nodules found on LDCT. The sensitivity of ULDCT was compared against the standard, and logistic regression analysis was used to determine the independent predictors for nodule detection.

Results: Compared with LDCT (0.93 ± 0.32 mSv), a 89.7% dose decrease was seen with ULDCT, for which the calculated effective dose was 0.096 ± 0.006 mSv ($P < 0.001$). LDCT showed 188 nodules, including 123 solid and 65 subsolid nodules. The overall sensitivity for nodule detection in ULDCT was 90.4% (170/188), and 98.2% (54/55) for nodules ≥ 6 mm. In multivariate analysis, nodule types and diameters were independent predictors of sensitivity ($P < 0.05$). However, patients' BMI had no effect on nodule detection ($P > 0.05$).

Conclusions: ULDCT can be used in the management of pulmonary nodules for people with BMI ≤ 30 kg/m^2 at 10% radiation dose of LDCT.

1. Introduction

Lung cancer is the most common cancer in the world and characterized by the highest mortality rate [1]. In 2016, 224000 new cases of lung cancer were reported in the United States, 60% of which were in the advanced stage [2]. Compared to the overall 5-year survival rate of 18% for lung cancer, the 5-year survival rate for non-small cell lung cancer can be obviously improved to 80% with appropriate treatment in the early stage [3,4]. Therefore, we believe lung cancer screening in the early stage to be significant. The National Lung Screening Trial in the United States has shown a relative risk reduction in death from lung cancer by 20% with low-dose computed tomography (LDCT) screening compared to that associated with plain-film chest radiography [5]. The maximum radiation dose of LDCT recommended by guidelines is 3 mSv for small people(BMI ≤ 30 kg/m^2), which is far higher than that recommended for plain-film chest radiography, 0.03–0.1 mSv [6,7]. In addition, a large number of indeterminate nodules need to be examined by follow-up evaluations with repeated LDCT to monitor for changes in diameter, which could result in an increase in the cumulative radiation dose that cannot be ignored [8–10]. Hence, lung cancer screening with ultralow-dose CT (ULDCT) has attracted great attention from radiologists.

In recent times, several strategies have been proposed to reduce the dose of ionizing radiation, including modification of tube potential and tube current and use of iterative reconstruction (IR). Reducing tube potential and tube current alone impairs image quality and lowers accuracies for radiologists. However, IR can obviously improve the image quality and reduce the noise at the same radiation exposure level, allowing for further reduction of the radiation dose [11,12].

Recently, a new IR technique adaptive statistical iterative reconstruction-V (ASiR-V, GE Healthcare, USA) was developed. ASiR-V can increase noise reduction performance over the original IR technique even at lower doses and it has been widely applied in phantom and clinical studies [13–15]. To the best of our knowledge, no data are available on ULDCT with ASiR-V for research on pulmonary nodules. Therefore, the purpose of this study was to investigate whether ULDCT with ASiR-V can be used for the detection and diameter measurement of pulmonary nodules at an extremely low dose comparable to those

* Corresponding author at: Department of Radiology, Peking University Third Hospital, 49 North Garden Road, Haidian District, Beijing, 100191, China.
E-mail address: huishy@bjmu.edu.cn (H. Yuan).

https://doi.org/10.1016/j.ejrad.2019.108652
Received 25 April 2019; Received in revised form 12 July 2019; Accepted 23 August 2019

associated with plain-film chest radiography. Furthermore, mixed-effects logistic regression analysis was used to determine independent predictors for the sensitivity of pulmonary nodule detection to explore the application range of ULDCT in Chinese patients.

2. Materials and methods

2.1. Patients

This single-center, prospective, observational study was approved by our hospital review board (clinicaltrials.gov identifier M2017217); informed consent was obtained from each participant. Between September 2017 and September 2018, 223 patients who underwent LDCT in our department were enrolled. The entry criteria for the study were (1) age > 18 years and BMI ≤ 30 kg/m^2; (2) fewer than four pulmonary nodules without calcification; (3) solid nodules (SNs) with a diameter of 4 ~ 15 mm and subsolid nodules (SSNs) with a diameter of 5 ~ 20 mm and containing part-solid nodules (PSNs) and ground-glass nodules (GGNs) (the diameter is the mean of the longest diameter and perpendicular diameter of a nodule); and (4) acceptable diagnostic image quality of LDCT. The Fleischner society guidelines 2017 were used as the nodule classification schema.

Thus, the final study population consisted of 188 patients (80 men, 108 women; mean age, 58.1 ± 15.3 years; age range 18 ~ 88 years; mean BMI, 23.6 ± 2.84 kg/m^2; BMI range, 16.41 ~ 29.87 kg/m^2).

2.2. CT protocol and image reconstruction

All examinations were performed using a 16 cm detector GE Revolution CT scanner (GE Healthcare, Milwaukee, WI, USA). All patients were scanned using the LDCT protocol. Then, doctor A (a radiologist with 4 years of experience in CT) would choose a nodule for local ULDCT in real-time at the acquisition time of LDCT. The criteria for choosing the nodules were as follows: SSNs were chosen first when both SNs and SSNs were present; after selection based on nodule type, nodules with the smaller diameter were selected. Thereafter, all patients underwent local ULDCT for the center of the chosen nodule detected on LDCT with 3-cm scan length range. The interval was less than 1 min bewteen LDCT and ULDCT.

For LDCT image acquisition, the usual clinical chest CT protocol was used in the helical mode: collimation of 64 × 0.625 mm, gantry rotation time of 0.28 s, Assist kV (120 /100 kV), 0.984:1 beam pitch, a z-axis tube current modulation with a noise index of 14.1 Hounsfield units (min/max mA, 50/680), and large body scan field of view (SFOV) and display field of view (DFOV) of 36 × 36 cm^2. For ULDCT image acquisition, all parameters remained unchanged, except that the tube potential was 120 kV, the tube current was lowered to 10 mA without dose modulation, and the scan range was 3 cm for the chosen nodule. LDCT and ULDCT images were reconstructed with ASiR-V at a level of 50% by using a slice thickness of 2.5 mm with an increment of 2.5 mm. The image matrix was 512 × 512 pixels.

2.3. CT data analysis

The dose parameters generated from LDCT protocols were recorded: the CT dose index-volume (CTDIvol), the dose-length product (DLP), and scan length (L). The CTDIvol for the ULDCT protocols was also recorded. According to the L of the LDCT examination, the DLP of the whole lung scanning range for the ULDCT protocol was calculated as followed: DLP = CTDIvol × L [16]. In order to compare the radiation dose of LDCT to ULDCT, we would calculate an effective dose (ED) for two scans. It was not calculated for each patient's actual radiation dose but only used to compare the two CT scan protocols. The ED for both CT scans was calculated by multiplying the DLP with a chest conversion coefficient (k: 0.014 mSv/mGy cm) [17].

Image noise was also assessed by measuring the standard deviation (SD) of regions of interest (ROI) placed by a radiologist doctor A. The ROI would be placed in the subcutaneous fat and paravertebral muscle at the ipsilateral level of the chosen nodule with the maximum diameter. The size of the ROI was 40 ~ 60 mm^2 and adjacent structures were avoided. The mean image noise was defined as the average of the SD in three consecutive ROIs at different z-axis positions.

The subjective axial image qualities of both LDCT and ULDCT were independently assessed by two radiologists (doctor B and doctor C, with 5 and 7 years of experience in radiology, respectively) who were blinded to the study design and all information regarding the patients. The window center and width of images were fixed to -600 Hu and 1600 Hu, respectively. The image qualities of the LDCT and ULDCT scans were graded on a modified 5-point Likert scale as previously shown [18]: 1 = nondiagnostic image quality, strong artefacts, insufficient for diagnostic purposes score; 2 = severe artefacts with uncertainty about the evaluation; 3 = moderate artefacts with restricted assessment; 4 = slight artefacts with unrestricted diagnostic image evaluation possible; and 5 = excellent image quality, no artefacts. Scans with a quality score of 3 to 5 were considered diagnostic. Images of the same lung segment on ULDCT were assessed in LDCT scans.

2.4. Assessment of pulmonary nodules

Four weeks after the evaluation of subjective image qualities, doctor B and doctor C independently performed the assessment of pulmonary nodules on LDCT. The location, type, and diameter of every nodule were recorded. In case discordance occurred in the identification of nodules, the final decision was made by doctor D (a radiologist with 20 years of experience in CT). The mean value of the nodule diameter measurements obtained by the two readers on LDCT was used for analyses. Another four weeks after the evaluation of nodules on LDCT, the same two readers evaluated the nodules on ULDCT. The results of ULDCT were separately recorded by the doctors. The results of LDCT were considered as the standards of reference.

2.5. Statistical analysis

Statistical analyses were performed using SPSS 20.0. A two-sided P-value of < 0.05 was considered statistically significant. Continuous variables were reported as mean ± SD, and categorical variables as frequencies or percentages. One-way ANOVA was used to compare the mean diameter and LSD-t test for comparison among groups; *t*-tests were used to compare DLP, ED, image noise, and subjective image quality scores. ULDCT sensitivity for nodule detection was determined along with 95% confidence intervals and compared using Chi-square statistics. To determine interobserver agreement for subjective image quality scores and sensitivity of nodule detection, the intraclass correlation coefficient (ICC) and kappa values were calculated. ICC values above 0.8, between 0.4 and 0.8, and under 0.4 indicate strong, moderate, and weak agreement, respectively. Kappa values above 0.75, between 0.40 and 0.75, and under 0.40 indicate strong, moderate, and weak agreement, respectively. Bland–Altman analysis was used to assess the agreement for nodule diameter measurements. Mixed-effects logistic regression was used to test for independent predictors for the sensitivity of pulmonary nodule detection.

3. Results

3.1. Radiation dose and image noise

Radiation dose of the two different protocols are summarized in Table 1. The ED of ULDCT (0.096 ± 0.006 mSv) was 89.7% lower than that of LDCT (0.93 ± 0.32 mSv; $P < 0.001$). Compared with LDCT images, the image noise of subcutaneous fat and paravertebral muscle on ULDCT images were both significantly lower ($P < 0.001$).

Table 1
Radiation dose and image noise.

	LDCT	ULDCT
L (cm), mean ± SD	35.91 ± 2.54(28.26 ~ 43.51)	NA
CTDIvol (mGy), $\bar{X}$ ± S	1.84 ± 0.60(1.02 ~ 4.11)	0.19
DLP (mGy × cm), $\bar{X}$ ± S,	66.29 ± 22.93(37.12 ~ 168.8)	6.87 ± 0.45(5.34 ~ 8.27)
ED (mSv), $\bar{X}$ ± S	0.93 ± 0.32(0.52 ~ 2.36)	0.096 ± 0.0006(0.075 ~ 0.116)
Paravertebral muscle (HU)	15.6 ± 2.4	21.1 ± 2.5
Subcutaneous fat (HU)	11.9 ± 1.3	19.6 ± 1.8

L, scan length; CTDIvol, CT dose index-volume; DLP, dose-length product; ED, effective dose; LDCT, low-dose computed tomography; ULDCT, ultralow-dose computed tomography; NA, not appropriate.

Table 2
Subjective image quality scores for both LDCT and ULDCT recorded by two doctors.

	LDCT		ULDCT	
	Doctor B	Doctor C	Doctor B	Doctor C
score = 5	165	158	0	0
4 ≤ score < 5	23	30	86	83
3 ≤ score < 4	0	0	99	102
score < 3	0	0	3	3

LDCT, low-dose computed tomography; ULDCT, ultralow-dose computed tomography.

3.2. Subjective image quality

The interobserver agreement was moderate for the assessment of subjective image quality on ULDCT (ICC of 0.534 [95% CI 0.379, 0.651]). The subjective image quality scores reported by two doctors for ULDCT were lower than those for LDCT (P < 0.001; Table 2). The proportion of ULDCT images with scores ≥ 3 (acceptable diagnostic quality) was 98.4%.

3.3. Detection of pulmonary nodules

Table 3 presents an overview of the nodules found on LDCT and ULDCT. The interobserver agreement was strong for nodule detection on ULDCT between two doctors (kappa = 0.914). Considering the good agreement, we decided to assess the performance of ULDCT for pulmonary nodule detection based on the results obtained by doctor B. On LDCT, 188 nodules were marked by two doctors in agreement, including 123 SNs and 65 SSNs (58 GGNs and 7 PSNs). On ULDCT, 184 nodules were marked, including 117 SNs and 67 SSNs (61GGNs and 6 PSNs). The overall sensitivity for nodule detection on ULDCT was 90.4% (170/188). For each type of nodules, the sensitivity was 94.3% (116/123) for SNs and 83.1% (54/65) for SSNs. For SNs, 7 of 123 nodules (5.7%) were misclassified as SSN with diameters below 5 mm. For SSNs, 10 of 65 nodules (15.4%) was missed on ULDCT and 1 of 65 nodules (1.5%) was misclassified as SN, which had a diameter of 5.8 mm. Nine of the 10 missed SSNs had diameters below 6 mm while one of them had a diameter of 9.1 mm. Only six SSNs were false positively detected on ULDCT. No nodules were seen on the corresponding area of LDCT.

Table 3
The detection of pulmonary nodules on LDCT and ULDCT.

ULDCT LDCT	SN	SSN	Not detected	Total number of nodules
SN	116	7	0	123
SSN	1	54	10	65
Not detected	0	6	0	NA
Total number of nodules	117	67	NA	184 188

LDCT, low-dose computed tomography; ULDCT, ultralow-dose computed tomography; SN, solid nodules; SSN, subsolid nodules; NA, not appropriate.

Table 4
Sensitivity for detection of pulmonary nodules of different diameters on ULDCT.

	4 ≤ diameter < 6 (mm)	6 ≤ diameter < 8 (mm)	Diameter > 8 (mm)	χ^2-value	P-value
SN	92.7% (89/96)	100% (20/20)	100% (7/7)	1.050	0.739
SSN	73.0% (27/37)*	100% (15/15)	92.3% (12/13)	6.112	0.032

ULDCT, ultralow-dose computed tomography; SN, solid nodule; SSN, subsolid nodule.
* the result of this group was lower than those of the two other groups.

The sensitivities for the detection of pulmonary nodules of different diameter on ULDCT are shown in Table 4. For SNs with diameter ≥ 4 mm, there were no differences among groups with different diameters (P > 0.05). However, for SSNs, the sensitivity for nodules with diameter ≥ 6 mm was significantly higher than that for nodules with diameter < 6 mm (P = 0.022). There was no significant difference between nodules with 6 mm ≤ diameter < 8 mm and nodules with diameters ≥ 8 mm (P > 0.05).

3.4. Measurement of pulmonary nodules

The agreement between interobserver's diameter measurements on ULDCT as well as agreement on LDCT and ULDCT are shown in Bland-Altman plots (Fig. 1A and B). In our study, the mean diameter of SNs in LDCT was 5.2 ± 1.6 mm (range 4.0 ~ 13.7 mm) and that of SSNs was 6.6 ± 2.0 mm (range 5.0 ~ 13.3 mm). The bias between two doctors on ULDCT was 0.04 mm and differences between diameters larger than 1 mm was found 0% of the time. Considering the good agreement between diameter measurements obtained by the two doctors on ULDCT, we chose the results of doctor B for the comparison. The bias between LDCT and ULDCT was 0.09 mm and differences between diameters larger than 1 mm was found 1.2% of the time.

3.5. Logistic regression for the predictors of nodule detection

The results of univariate and multivariate analysis for the predictors of nodule detection in our study are presented in Table 5. Univariate analysis showed that nodule type and diameter were the predictors for the sensitivity of nodule detection (P = 0.013 and P = 0.016, respectively). Meanwhile, the results of the multivariate analysis came to the same conclusion.

4. Discussion

In this study, we aimed to investigate whether ULDCT with ASiR-V could be used for the detection and diameter measurement of pulmonary nodules at the extremely low doses comparable to those used in plain film chest radiography. We also aimed to explore the application range of ULDCT for pulmonary nodule detection in Chinese people.

As a new IR technique, ASiR-V employs a system physics model

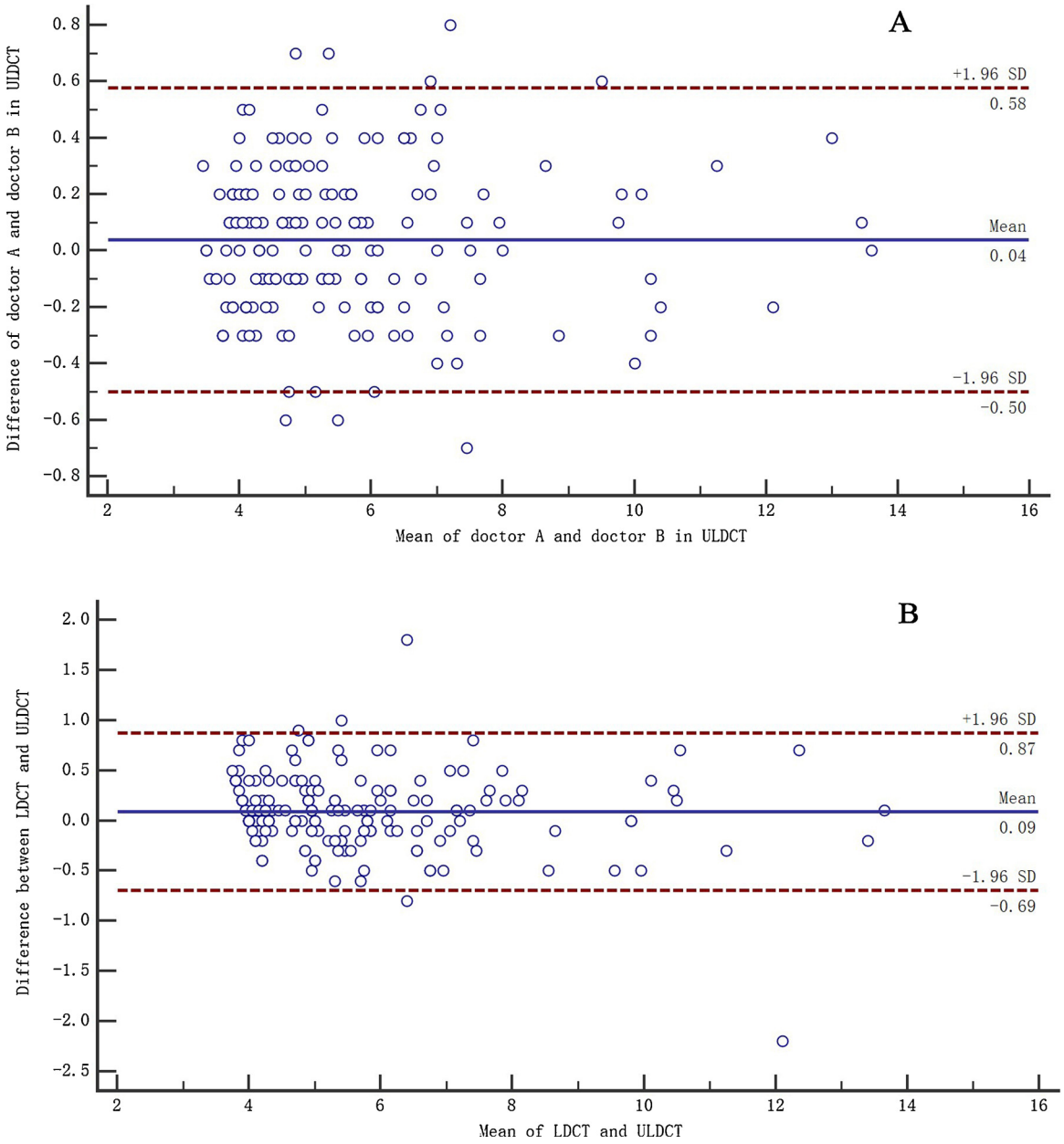

Fig. 1. Bland–Altman plots of diameter measurement. (A) Diameter measurement analysis between doctor A and doctor B, and (B) diameter measurement analysis between LDCT and ULDCT.

from the model-based iterative reconstruction algorithm and an enhanced noise model in comparison with ASIR [19,20]. Therefore, ASiR-V has a fast reconstruction speed and the same ability to reduce noise at lower radiation doses, allowing further reduction of the radiation dose. Some recent reports have described the application of ULDCT with IR in lung cancer screening; in those studies, the ED was 0.13–0.49 mSv [21–25]. In our study, the ED of ULDCT with ASiR-V was 0.096 mSv, which was, to our knowledge, the lowest reported value and was similar to the radiation dose of plain film chest radiography (0.03-0.1 mSv) [6]. The ED of ULDCT was 89.7% lower than that of LDCT (0.93 mSv). However, the proportion of scans with image quality that was considered diagnostic was as high as 98.4% (185/188). Our results indicated that ASiR-V can provide much higher dose reduction than the 22%–48% dose reduction obtained with ASiR [26]. we concluded that the image quality of ULDCT reconstructed with ASiR-V can meet the diagnostic requirements for pulmonary nodule detection. The overall sensitivity for nodule detection in our study was 90.4%. Even with the 89.4% dose reduction in comparison with LDCT, the sensitivity for nodule detection of ULDCT decreased by less than 10%. The representative cases for LDCT and ULDCT are shown in Figs. 2 and 3.

In lung cancer screening, the nodule type and diameter are the most important factors influencing the management strategies, and treatment differs significantly for nodules with different diameters [27]. In our study, the mean value of measurement of pulmonary nodules between ULDCT and LDCT was less than 0.1 mm. The proportion of nodules with differences between diameters less than 1 mm was as high as 98.8%. The biggest difference between diameters was 2.2 mm and this nodule was SSN with diameter of 11 mm. In summary, our study results still indicated a good agreement between the diameter measurements obtained with LDCT and ULDCT. A previous study on SN diameter measurement using ULDCT with SAFIRE reconstruction expressed the same view [24]. Considering these facts, we thought that ULDCT is an effective method for measurement of the diameter of pulmonary nodules.

Table 5
Univariate and multivariate analysis of the predictors of nodule detection on ULDCT.

		Univariate analysis			Multivariate analysis[c]		
					Full model		
		Correctly detected*	Not correctly detected&	P-value	Regression coefficient	OR-value	P-value
Nodule type	SN	94.3%	5.7%	0.013[a]	2.195	8.981	0.001[d]
	SSN	83.1%	16.9%				
Diameter (mm)	SN	5.3 ± 1.6	4.2 ± 0.2	0.000[b]	0.778	2.1777	0.023[d]
	SSN	6.8 ± 2.1	5.6 ± 1.2	0.016[b]			
BMI (kg/m^2)	SN	23.8 ± 2.9	24.5 ± 3.2	0.525[b]	−0.118	0.889	0.220[d]
	SSN	23.1 ± 2.7	23.9 ± 2.9	0.374[b]			

ULDCT, ultralow-dose computed tomography; BMI, body mass index; SN, solid nodule; SSN, subsolid nodule.
Correctly detected*, includes true positive results; Not correctly detected&, includes false positive and false negative results.
[a] Chi-squared test.
[b] t-test.
[c] mixed effects logistic regression modeling for detection of nodules as a linear combination of all predictor variables as a full model.
[d] likelihood-ratio tests.

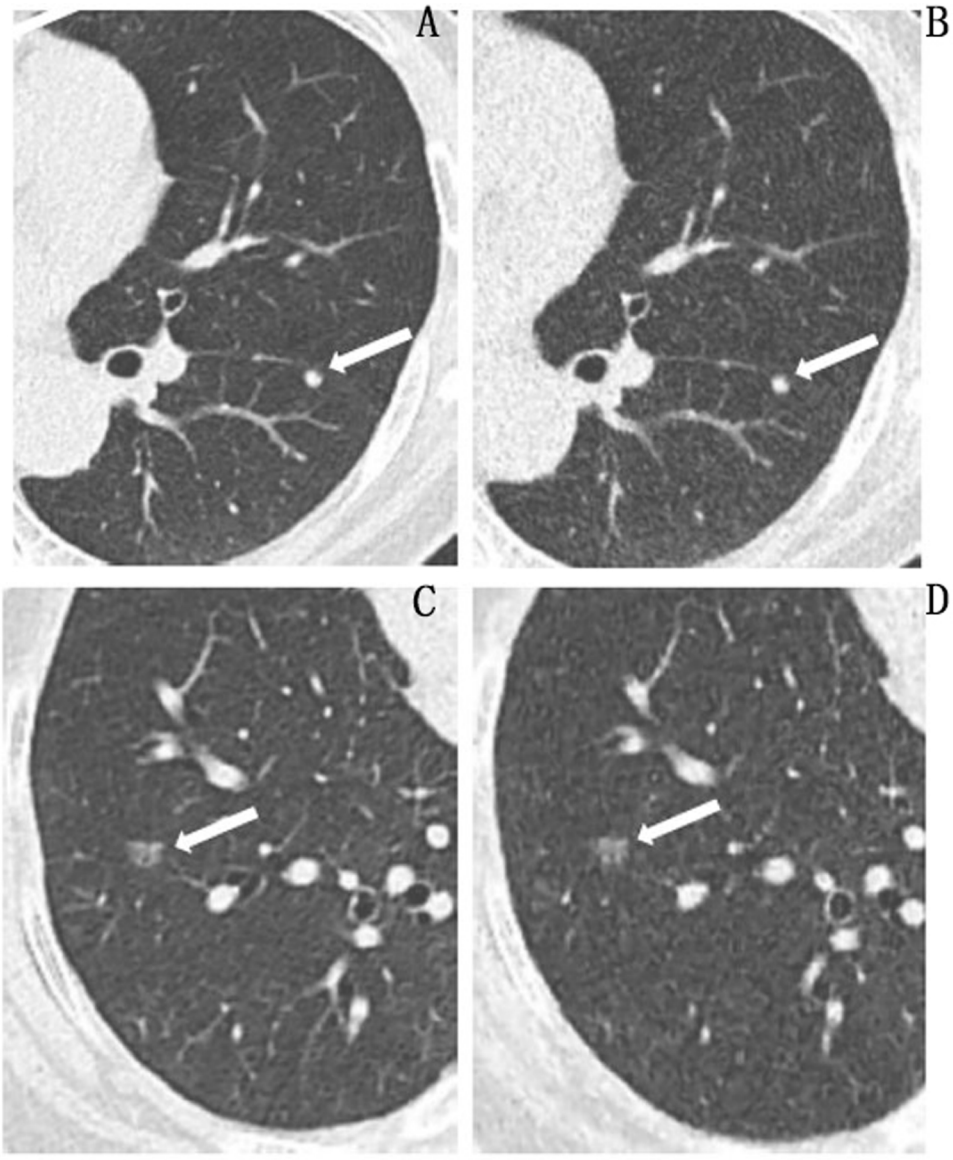

Fig. 2. Transverse CT sections of the lung in a 18-year-old man with a body mass index of 20.96 kg/m^2 scanned with low dose (A) (effective dose, 0.66 mSv; CTDIvol, 1.30 mGy) and ultralow dose (B) (effective dose, 0.099 mSv; CTDIvol, 0.19 mGy). The solid pulmonary nodule in the left lower lobe with a dimeter of 4.7 mm was detected in ultralow-dose CT by both readers. Transverse CT sections of the lung in a 82-year-old woman with a body mass index of 20.0 kg/m^2 scanned with low dose (A) (effective dose, 0.77mSv; CTDIvol, 1.68 mGy) and ultralow dose (B) (effective dose, 0.087 mSv; CTDIvol, 0.19 mGy). The subsolid pulmonary nodule with a dimeter of 6.1 mm in the right lower lobe was detected in ultralow-dose CT by both readers.

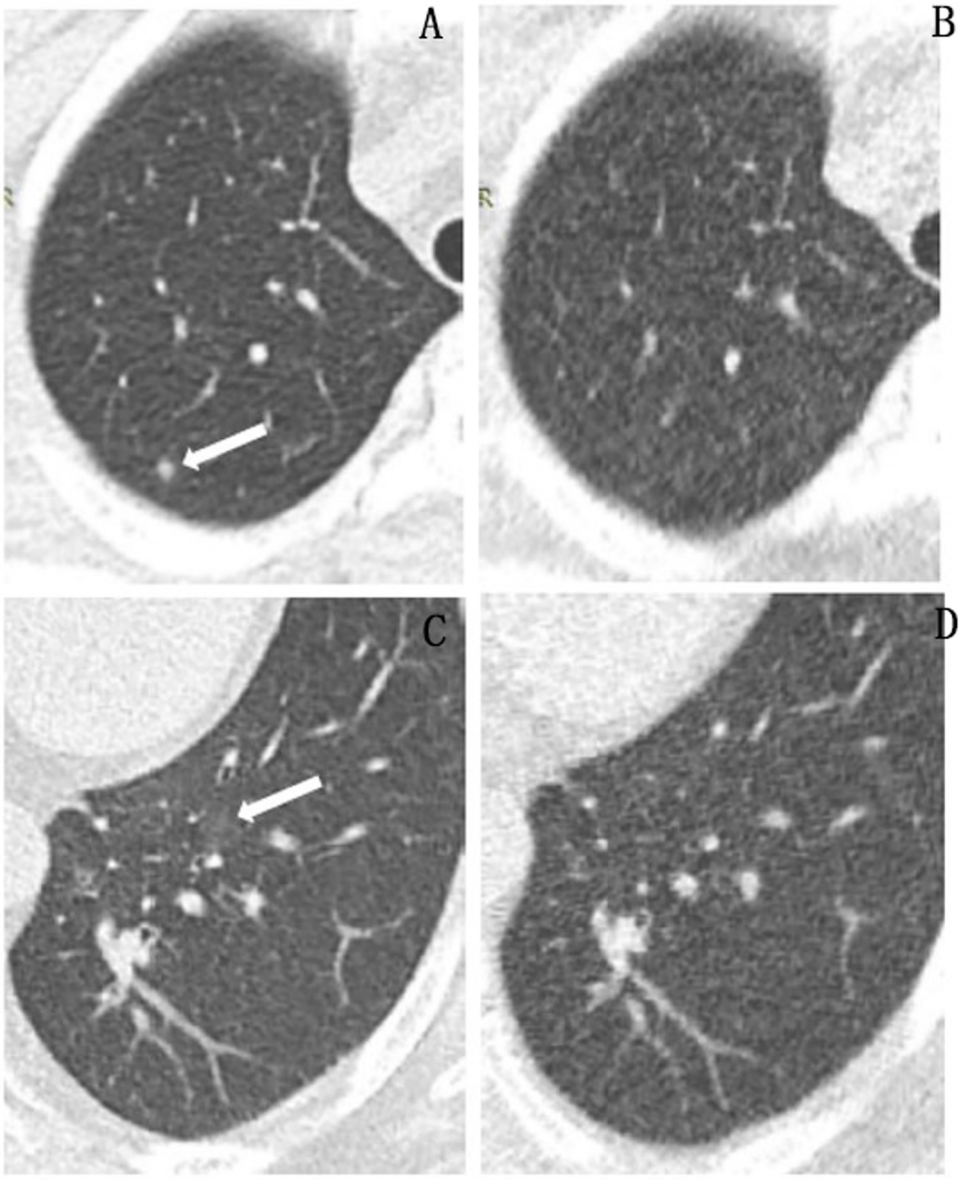

Fig. 3. Transverse CT sections of the lung in a 33-year-old woman with a body mass index of 25.0 kg/m^2 scanned with low dose (A) (effective dose, 0.84 mSv; CTDIvol, 1.82 mGy) and ultralow dose (B) (effective dose, 0.088 mSv; CTDIvol, 0.19 mGy). The solid pulmonary nodule with a dimeter of 4.0 mm in the right upper lobe was not detected in ultralow-dose CT by both readers. Transverse CT sections of the lung in a 56-year-old woman with a body mass index of 26.83 kg/m^2 scanned with low dose (A) (effective dose, 0.95mSv; CTDIvol, 2.05 mGy) and ultralow dose (B) (effective dose, 0.090 mSv; CTDIvol, 0.19 mGy). The subsolid pulmonary nodule with a dimeter of 9.1 mm in the left lower lobe was not detected in ultralow-dose CT by both readers.

According to the results of the multivariate and univariate analyses, nodule diameter and type were the independent predictors for nodule detection. Moreover, patient BMI had no significant effect on nodule detection. The sensitivity for SNs was 94.3% and was obviously higher than that for SSNs (83.1%; $P < 0.05$). This can be explained easily by the higher density of SNs.

The diameter of pulmonary nodules was also an independent predictor for nodule detection. The sensitivity of pulmonary nodule detection increased markedly with an increase in the diameter. However, the influence differed across nodule types. For SNs, the sensitivity was 92.7% for nodules with 4 mm ≤ diameter < 6 mm and 100% for nodules with diameter ≥6 mm. There was no obvious difference between the sensitivities for these two diameter-based groups ($P > 0.05$). The result indicated that the sensitivity for SNs with diameter ≥4 mm in ULDCT was extremely high and would not be influenced significantly by changes in nodule size. For SSNs, the results were markedly different. The sensitivity for SSNs with diameter < 6 mm was 73.0%. However, the sensitivity for SSNs with diameter ≥6 mm increased remarkably to 96.4% ($P < 0.05$). The only one missed nodule among the 28 SSNs with diameter ≥6 mm was located in the left lower lobe and behind the heart. The CT value of this nodule was as low as −710 Hu. The reason for being missed may be explained by the fact that the density of this nodule was too low (the mean CT value of truly detected SSNs was −560 Hu), and the poor image quality because of the coverage by the heart (Fig. 3). There were only six SSNs detected on ULDCT but not found on LDCT. The false positive rate was as low as 3.3%. The rate of misclassification for SNs was 5.6% and 1.5% for SSNs.

Although the sensitivity for SSNs with diameter < 6 mm was slightly low, the sensitivity for nodules with diameter ≥6 mm was still above 95% for both SNs and SSNs. All of these data indicated that ULDCT showed high sensitivity for the detection of pulmonary nodules with diameter longer than 6 mm. In the previous study by Messerli, the sensitivity for detection of SNs and SSNs with diameter ≥ 6 mm was 99% and 95%, which was the same as our results [22]. However, the radiation dose of ULDCT in our study was 0.096 mSv, which was 26.2% lower than the 0.13mSv dose reported by Messerli. The risk for malignancy of pulmonary nodules will increase obviously with longer diameters. However, the risk for malignancy of nodules smaller than 6 mm is very low and the Fleischner society guidelines 2017 even recommended no routine follow-up for nodules smaller than 6 mm [10]. In general, 80% was the minimally acceptable sensitivity for screening trials [28]. Considering the fact that the sensitivity for nodules with

diameter ≥6 mm was above 95%, we think that ULDCT scans can meet the sensitivity requirement for pulmonary nodule detection in clinical practice.

It is generally believed that the image quality will worsen with an increase in patient BMI under the a fixed CT scan protocol. Therefore, the sensitivity of ULDCT for pulmonary nodules will decrease. However, our study yielded contrasting findings. In both multivariate and univariate analyses, the patients' BMI had no significant effects on the detection rate of SNs and SSNs ($P > 0.05$). Our results are distinct from those of another study that investigated the detection rate of pulmonary nodules in reduced-dose thoracic CT [29]. The range of patients' BMI values in that report was larger and the maximum value was larger than 45.1 kg/m^2. However, the BMI values in our study were all less than 30 kg/m^2. The smaller BMI values may explain the difference in our findings. Thus, we can conclude that the BMI of patients has no obvious effects on the detection rate of pulmonary nodules when the BMI values are less than 30 kg/m^2.

There are some limitations of our study. First, our ULDCT examination didn't include the entire volume of the lungs and therefore we could not assess the quality of the images and false positivity in their entirety. Second, no true negative control groups were set up in this study and all patients in our study had pulmonary nodules. So, specificity cannot be evaluated in our study as specificity = true negative/(true negative + false positive). However, the false positive rate was as low as 3.2%, indicating the potential high specificity of ULDCT. Third, the diameter range for SNs was 4.0 ~ 15 mm and that for SSNs was 5.0 ~ 20 mm. Considering the fact that the guidelines recommended no routine follow-up for nodules smaller than 6 mm and SNs with diameter > 15 mm can be easily detected in the plain film chest radiographs, the chosen diameter range of nodules in our study was acceptable. Fourth, the BMI values in our study were all less than 30 kg/m^2, and patients with BMI > 30 are not covered. Considering the fact that the BMI of Chinese people is smaller than those of people in Western countries and the lower obesity rate, we only chose patients who did not meet the criteria for obesity (BMI < 30 kg/m^2). Further studies should aim to recruit more patients with larger BMI, and pulmonary nodules of different diameters should be included to test the detection efficiency of ULDCT in the entire volume of the lungs, especially the specificity of ULDCT for nodule detection.

5. Conclusion

In summary, our study results indicate that ULDCT with ASiR-V reconstruction can obviously improve the image quality and provide extremely high sensitivity for nodule detection along with good diameter measurement accuracy at very low radiation dose. Hence, we recommend that ULDCT can be used in the management of pulmonary nodules for people with BMI ≤ 30 kg/m^2.

Declaration of Competing Interest

The authors have no conflict of interest.

References

[1] L.A. Torre, R.L. Siegel, E.M. Ward, A. Jemal, Global cancer incidence and mortality rates and trends–An update, Cancer Epidemiol. Biomarkers Prev. 25 (2016) 16–27, https://doi.org/10.1158/1055-9965.EPI-15-0578.

[2] R.L. Siegel, K.D. Miller, A. Jemal, Cancer statistics, 2016, CA Cancer J. Clin. 66 (2016) 7–30, https://doi.org/10.3322/caac.21332.

[3] S.R. Carr, M.J. Schuchert, A. Pennathur, et al., Impact of tumor size on outcomes after anatomic lung resection for stage 1A non-small cell lung cancer based on the current staging system, J. Thorac. Cardiovasc. Surg. 143 (2012) 390–397, https://doi.org/10.1016/j.jtcvs.2011.10.023.

[4] A. Noone, N. Howlader, M. Krapcho, et al., SEER Cancer Statistics Review, 1975-2015, Based on November 2017 SEER Data Submission, Posted to the SEER Web Site, April 2018 National Cancer Institute, Bethesda, MD, 2018https://seer.cancer.gov/csr/1975_2015/.

[5] D.R. Aberle, A.M. Adams, C.D. Berg, et al., Reduced lung-cancer mortality with low-dose computed tomographic screening, N. Engl. J. Med. 365 (2011) 395–409, https://doi.org/10.1056/NEJMoa1102873.

[6] E. Quaia, E. Baratella, S. Cernic, et al., Analysis of the impact of digital tomosynthesis on the radiological investigation of patients with suspected pulmonary lesions on chest radiography, Eur. Radiol. 22 (2012) 1912–1922, https://doi.org/10.1007/s00330-012-2440-3.

[7] P.B. Bach, J.N. Mirkin, T.K. Oliver, et al., Benefits and harms of CT screening for lung cancer: a systematic review, JAMA 307 (2012) 2418–2429, https://doi.org/10.1001/jama.2012.5521.

[8] L.H. Schmidt, B. Vietmeier, G. Kaleschke, et al., Thoracic malignancies and pulmonary nodules in patients under evaluation for transcatheter aortic valve implantation (TAVI): incidence, follow up and possible impact on treatment decision, PLoS One 11 (2016) e0155398, , https://doi.org/10.1371/journal.pone.0155398.

[9] D.P. Blagev, J.F. Lloyd, K. Conner, et al., Follow-up of incidental pulmonary nodules and the radiology report, J. Am. Coll. Radiol. 11 (2014) 378–383, https://doi.org/10.1016/j.jacr.2015.12.008.

[10] H. MacMahon, D.P. Naidich, J.M. Goo, et al., Guidelines for management of incidental pulmonary nodules detected on CT images: from the Fleischner society 2017, Radiology 284 (2017) 228–243, https://doi.org/10.1148/radiol.2017161659.

[11] T. Kubo, Y. Ohno, H.U. Kauczor, H. Hatabu, Radiation dose reduction in chest CT–review of available options, Eur. J. Radiol. 83 (2014) 1953–1961, https://doi.org/10.1016/j.ejrad.2014.06.033.

[12] H.J. Kim, S.Y. Yoo, T.Y. Jeon, J.H. Kim, Model-based iterative reconstruction in ultra-low-dose pediatric chest CT: comparison with adaptive statistical iterative reconstruction, Clin. Imaging 40 (2016) 1018–1022, https://doi.org/10.1016/j.clinimag.2016.06.006.

[13] M. Gatti, F. Marchisio, M. Fronda, et al., Adaptive statistical iterative reconstruction-V versus adaptive statistical iterative reconstruction: impact on dose reduction and image quality in body computed tomography, J. Comput. Assist. Tomogr. 42 (2018) 191–196, https://doi.org/10.1097/RCT.0000000000000677.

[14] C.W. Chen, P.A. Chen, C.C. Chou, et al., Combination of adaptive statistical iterative Reconstruction-V and lower tube voltage during craniocervical computed tomographic angiography yields better image quality with a reduced radiation dose, Acad. Radiol. (2018) 1–8, https://doi.org/10.1016/j.acra.2018.07.019.

[15] M. Afadzi, E.K. Lysvik, H.K. Andersen, ACT M, Ultra-low dose chest computed tomography: Effect of iterative reconstruction levels on image quality, Eur. J. Radiol. 114 (2019) 62–68, https://doi.org/10.1016/j.ejrad.2019.02.021.

[16] V.A. Murugan, M.K. Kalra, M. Rehani, S.R. Digumarthy, Lung Cancer screening: computed tomography radiation and protocols, J. Thorac. Imaging 30 (2015) 283–289, https://doi.org/10.1097/RTI.0000000000000150.

[17] P.D. Deak, Y. Smal, W.A. Kalender, Multisection CT protocols: sex- and age-specific conversion factors used to determine effective dose from dose-length product, Radiology 257 (2010) 158–166, https://doi.org/10.1148/radiol.10100047.

[18] P. Prakash, M.K. Kalra, J.B. Ackman, et al., Diffuse lung disease: CT of the chest with adaptive statistical iterative reconstruction technique, Radiology 256 (2010) 261–269, https://doi.org/10.1148/radiol.10091487.

[19] H.G. Kim, H.J. Lee, S.K. Lee, H.J. Kim, M.J. Kim, Head CT, Image quality improvement with ASIR-V using a reduced radiation dose protocol for children, Eur. Radiol. 27 (2017) 3609–3617, https://doi.org/10.1007/s00330-017-4733-z.

[20] P. Ning, S. Zhu, D. Shi, Y. Guo, M. Sun, X-ray dose reduction in abdominal computed tomography using advanced iterative reconstruction algorithms, PLoS One 9 (2014) e92568, , https://doi.org/10.1371/journal.pone.0092568.

[21] Y. Ohno, K. Aoyagi, Q. Chen, et al., Comparison of computer-aided detection (CADe) capability for pulmonary nodules among standard-, reduced- and ultra-low-dose CTs with and without hybrid type iterative reconstruction technique, Eur. J. Radiol. 100 (2018) 49–57, https://doi.org/10.1016/j.ejrad.2018.01.010.

[22] M. Messerli, T. Kluckert, M. Knitel, et al., Ultralow dose CT for pulmonary nodule detection with chest x-ray equivalent dose - a prospective intra-individual comparative study, Eur. Radiol. 27 (2017) 3290–3299, https://doi.org/10.1007/s00330-017-4739-6.

[23] M. Fujita, T. Higaki, Y. Awaya, et al., Lung cancer screening with ultra-low dose CT using full iterative reconstruction, J. Radiol. 35 (2017) 179–189, https://doi.org/10.1007/s11604-017-0618-y.

[24] X. Sui, F.G. Meinel, W. Song, et al., Detection and size measurements of pulmonary nodules in ultra-low-dose CT with iterative reconstruction compared to low dose CT, Eur. J. Radiol. 85 (2016) 564–570, https://doi.org/10.1016/j.ejrad.2015.12.013.

[25] M. Paks, P. Leong, P. Einsiedel, L.B. Irving, D.P. Steinfort, D.M. Pascoe, Ultralow dose CT for follow-up of solid pulmonary nodules: a pilot single-center study using Bland-Altman analysis, Medicine (Baltimore) 97 (2018) e12019, https://doi.org/10.1097/MD 0000000000012019.

[26] F.A. Miéville, F. Gudinchet, F. Brunelle, F.O. Bochud, F.R. Verdun, Iterative reconstruction methods in two different MDCT scanners: physical metrics and 4-alternative forced-choice detectability experiments–a phantom approach, Phys. Med. 29 (2013) 99–110, https://doi.org/10.1016/j.ejmp.2011.12.004.

[27] D.S. Ettinger, D.E. Wood, D.L. Aisner, et al., Non-small cell lung cancer, version 5.2017, NCCN clinical practice guidelines in oncology, J. Compr. Canc. Netw. 15 (2017) 504–535 https://ghr.nlm.nih.gov/condition/lung-cancer.

[28] D.L. Miglioretti, L. Ichikawa, R.A. Smith, et al., Criteria for identifying radiologists with acceptable screening mammography interpretive performance on basis of multiple performance measures, AJR Am. J. Roentgenol. 204 (2015) W486–491, https://doi.org/10.2214/AJR.13.12313.

[29] V. Vardhanabhuti, C.L. Pang, S. Tenant, J. Taylor, C. Hyde, C. Roobottom, Prospective intra-individual comparison of standard dose versus reduced-dose thoracic CT using hybrid and pure iterative reconstruction in a follow-up cohort of pulmonary nodules-Effect of detectability of pulmonary nodules with lowering dose based on nodule size, type and body mass index, Eur. J. Radiol. 91 (2017) 130–141, https://doi.org/10.1016/j.ejrad.2017.04.006.